TÜBİTAK

Turkish Journal of Physics

http://journals.tubitak.gov.tr/physics/

Research Article

Turk J Phys
(2013) 37: 132 – 144
© TÜBİTAK
doi:10.3906/fiz-1112-12

Molecular dynamic simulation on iron corrosion-reduction in high temperature molten lead-bismuth eutectic

Artoto ARKUNDATO[1,2*], Zaki SU'UD[1], Mikrajuddin ABDULLAH[1], Widayani SUTRISNO[1]

[1]Department of Physics, Bandung Institute of Technology, Jalan Ganesha 10, Bandung 40132, Indonesia
[2]Department of Physics, Jember University, East Java, Indonesia

Received: 26.12.2011 • **Accepted:** 23.07.2012 • **Published Online:** 20.03.2013 • **Printed:** 22.04.2013

Abstract: Molecular dynamic simulation on iron in high-temperature molten lead-bismuth eutectic has been carried out to investigate the iron corrosion and its mitigation. The aim of the work is to investigate the corrosion and evaluate proper oxygen content of injection for significant and effective reduction. To study the phenomena we calculated the diffusion coefficients, radial distribution functions and mean square displacement of iron, and also observed the microstructure of iron before and after oxygen injection into coolant. The present calculation shows that a significant and effective reduction of corrosion can be achieved by injection of 7.68×10^{-2}–1.55×10^{-1} wt% into coolant at temperature 750 °C. It is predicted that the lower limit of oxygen content, 7.68×10^{-2} wt%, is the minimum value to develop a self-healing stable protective oxide film for preventing high dissolution of iron; and that the upper limit of oxygen content, 1.55×10^{-1} wt%, is the maximum value in order to avoid the precipitation of coolant oxides. By injection of 7.68×10^{-2} wt% of oxygen, the corrosion rate has been reduced about 92.16% at 750 °C, and reduced by 98.66% at the lower temperature 550 °C, compared with the normal, oxygenless condition.

Key words: Corrosion of pure iron, lead-bismuth eutectic, molecular dynamic, diffusion, oxygen content

1. Introduction

It has been known that the lead-bismuth eutectic (LBE) is an important coolant candidate for advanced nuclear-reactors design. This coolant has advantage properties such as low melting temperature (∼125.1 °C), high boiling temperature (∼1670 °C) and chemical stability [1–3]. However, it is also well known that the fuel cladding of the reactor is severely corroded due to its interaction with high temperature molten LBE [3–6]. The LBE has high solubility for iron, chromium and especially nickel at high temperatures. Since solubility is temperature dependent, the LBE tends to dissolve the structural materials (cladding) in the hot sections of the system and precipitate it in the cold sections of the system, clogging the piping [7]. This problem has brought critical challenges, i.e. how to reduce the corrosion rate and/or how to design novel corrosion-resistant materials. The corrosion process must be understood, controlled and reduced for safety and economic reasons.

One technique to reduce the corrosion is to develop a stable oxide scale (self-healing protective films) on the structural materials (cladding, pipe, vessel system, etc.) surfaces to prevent direct dissolution of metal components by maintaining the necessary concentration of dissolved oxygen in the LBE coolant [5, 7–11]. This protective oxide reduces the dissolution of structural materials into LBE, since the material components

*Correspondence: a_arkundato@students.itb.ac.id

must first pass through the oxide films [7]. The active oxygen control in lead or LBE coolant can bring to acceptable low corrosion rates and help prevent slag formation and plugging. Experiments show that the oxygen concentration was controlled within the range between formation of magnetite Fe_3O_4 layers and formation of PbO oxide [12]. To control the concentration of oxygen dissolved in LBE, a sensor for measuring oxygen activity is required [9]. However, it is impossible in an operating reactor to visually inspect the surface condition of materials to verify that oxide is present hence protecting those structural materials [7].

Although many corrosion experiments had been reported [3–12], a method to completely and effectively handle the corrosion is still needed. In addition, it is not easy to do the corrosion experiments in an operating reactor. To overcome this difficulty, computational methods have become an important way to study and predict the phenomena. In the present work we use the method of molecular dynamics (MD) [13–17]. Maulana et al. have used MD to investigate penetration depth of Pb and Bi atoms into iron material [15]. This type of corrosion was investigated based using the Lennard-Jones potential. However, in their preliminary study, they did not study the corrosion phenomena based on the diffusion coefficient calculation and also they did not address the reduction mechanism. In previous [14] and current work, we study the corrosion and its reduction based on the diffusion coefficient calculation. We continue with the Lennard-Jones potential for simple MD simulations, with potential parameters taken from experimental data (see Table).

Table. The Lennard-Jones potential parameters that were used in the present work.

Pair Interaction	σ (Å)	ε (eV)	Pair Interaction	σ (Å)	ε (eV)
Fe-Fe	0.400	2.319	Fe-Pb	0.277	2.754
Pb-Pb	0.191	3.189	Fe-Bi	0.154	2.685
Bi-Bi	0.059	3.050	Fe-O	0.064	2.784
O-O	0.010	3.428	Pb-Bi	0.106	3.119
Bi-O	0.025	3.149	Pb-O	0.044	3.218

Soontrapa and Chen [16] used the Embedded Atomic Method (EAM) potential for MD simulation to describe the atomic interaction for metal/metal oxide systems. They continued the study using the EAM potential to model the iron oxidation during magnetite development [17]. However, they did not study the corrosion based on the coefficient diffusion calculation as we have in our work.

Experimental studies show that temperature, oxygen concentration, flow velocity of coolant, material composition and thermal gradient play important roles in the corrosion process [12]. In our work, we studied the corrosion based on the temperature and oxygen concentration variations. Via molecular dynamic simulation, we have developed a quantitative and qualitative conclusion for using oxygen injection as a reduction technique in LBE iron corrosion. In our simulation model the corrosion was studied by assumption that the corrosion is mainly the result of iron dissolution [5]. For safe application, corrosion-resistant materials must be usable not only under normal condition but also under temporary anomalous conditions.

Rivai and Takahashi have communicated that the cladding temperature of lead alloy-cooled fast reactors can suddenly rise up to near 800 °C for several minutes to hours, under abnormal (accidental) conditions. The maximum temperature of cladding can reach 792 °C due to ULOHS (unprotected Loss of Heat Sink)/ULOF (unprotected Loss of Flow) [18]. Rivai and Takahashi [19] have also reported the corrosion behavior of Al-Fe coated steel in molten LBE at a temperature of 700 °C [19].

Based on these important pictures, and based on the availability of experimental data [5], we focus our study on simulations at temperature 750 °C. As a preliminary study, we explore the pure iron material (major

component of steels). The aims of the study is then:

- to investigate the corrosion of iron in high temperature stagnant molten LBE ($>$ 500 °C);
- to evaluate proper oxygen content of injection for significant and effective reduction of iron corrosion.

2. Theoretical background

2.1. Interatomic potential

Molecular dynamic is a simulation method where under certain condition the atoms of the system are allowed to evolve for a specified period of time and then the atomic trajectories are able to be evaluated via Newton's 2^{nd} law of motion:

$$\vec{F}_i = \nabla U = m_i \frac{d^2 \vec{r}_i}{dt^2}, \tag{1}$$

where U is potential energy of the system, $\overline{r}_i$ is the position of atom i, m_i is the mass of atom i, and t is time. We used the Lennard-Jones (LJ) n-m potential for interaction of all particles [20]:

$$U(r) = k\varepsilon \left[\left(\frac{\sigma}{r}\right)^n - \left(\frac{\sigma}{r}\right)^m \right], \tag{2}$$

where σ and ε are the LJ potential parameters. Coefficient $k$specifies the potential function:

$$k = \frac{n}{n-m} \left(\frac{n}{m}\right)^{m/(n-m)}. \tag{3}$$

Values n = 2 and m = 12 give the popular LJ potential of the form

$$U(r) = 4\varepsilon \left[\left(\frac{\sigma}{r}\right)^{12} - \left(\frac{\sigma}{r}\right)^{6} \right]. \tag{4}$$

To maintain the validation of LJ potentials we used the Fe-Fe and Pb-Pb pairs interaction as reported by Zhen and Davies [20], O-O interaction by Lemmon and Jacobsen [21] and Bi-Bi interaction from fitting of the EAM pair potential [22]. Cross-interactions (Fe-Pb, Fe-O and Pb-O) were approached by using the popular Lorentz-Berthelot mixing formula:

$$\sigma_{AB} = \frac{(\sigma_{AA} + \sigma_{BB})}{2} \tag{5a}$$

$$\varepsilon_{AB} = \sqrt{\varepsilon_{AA} \cdot \varepsilon_{BB}} \tag{5b}$$

The LJ parameters used in our simulation can be seen as in the Table. To get all trajectories of atoms we solved the Newton equation (1) using the MOLDY molecular dynamic program [14–17, 23, 24]. This code is an open-source package program, easy to operate for producing the thermodynamics quantities and can be used for liquids, solids and also gases studies.

2.2. Corrosion and diffusion coefficient

Corrosion may be defined as a degradation of structural materials into its constituent atoms. Generally, corrosion denotes transfer of electrons due to chemical reactions. However for liquid metal corrosion this definition should be broadened to the formation of solution of solid metal in a liquid metal due to solubility of the solid metal,

where *no* transfer of electrons is involved [25]. Solubility of iron, chromium and nickel in lead, bismuth and LBE plays an important role in corrosion phenomena when using heavy liquid metals (e.g. LBE) as a coolant [5, 7]. During operation of nuclear reactors, the fission reactions in the fuel, inside the cladding, produce the high heat, hence high temperatures in which the cladding material resides. At high temperature there is high solubility of metal elements Ni, Cr but mainly Fe in high temperature molten LBE leading to high corrosion [7, 9, 18]. This is a hot, non-galvanic type corrosion [25]. Furukara et al. communicated that solubility of iron, nickel and chromium was higher in LBE than in other liquid metal-sodium solutions [26]. Gromov et al. reported that the solubility of Ni, Cr and Fe in LBE could be formulated as $\log C_{Ni} = 1.53 - 843/T$, $\log C_{Cr} = -0.02 - 2280/T$ and $\log C_{Fe} = 2.01 - 4.380/T$, respectively [27].

Based on the above descriptions, in our work the corrosion is treated as a pure diffusion process without chemical reaction or transfer of electrons. We focus on the diffusion of iron in molten LBE. To evaluate the corrosion by dissolution of iron, we use three equations: the mean square displacement, MSD, the popular Einstein relation of diffusion coefficient, D, and the general Arrhenius formula, $D(T)$, as shown in the following equations, respectively [28]:

$$MSD = \langle \vec{r}(t) - \vec{r}(t=0)|^2 \rangle, \tag{6}$$

$$D = \lim_{t\to\infty} \frac{\langle \vec{r}(t) - \vec{r}(t=0)|^2 \rangle}{6t}, \tag{7}$$

$$D\,(T) = D_0 exp\left(-\frac{A}{R}\cdot\frac{1}{T}\right). \tag{8}$$

Here, T is temperature, $R = 8.314$ Jmol^{-1}K^{-1} is the universal gas constant, and A is activation energy for diffusion to be happened.

3. Simulation details

The MD simulation was applied to study the atomic interactions of iron, coolant and oxygen. The iron diffusion coefficients are calculated from simulations to explain the corrosion phenomena and effects of oxygen injection into coolant. To realize our work we divided our simulations as the below steps.

3.1. Iron diffusion calculation without oxygen content

The first simulation is to calculate $D(T)_{0wt\%}$, the temperature dependence of iron diffusion coefficient in LBE that represents the normal corrosion before mitigation effort by injecting oxygen. The first simulation is also meant to check the validity of the corrosion simulation model. The simulation is initiated with the arrangement of 1729 iron atoms in bcc crystal (with lattice constant 2.8286 Å and atomic mass 55.847 a.m.u), placed in the centre of coolant, as shown in Figure 1. The LBE coolant has density 0.0274 atoms/Å^3 that composed of 2540 ($\sim$45wt%) lead and 3037 ($\sim$55wt%) bismuth. The atomic mass of lead and bismuth are 207.19 a.m.u and 208.98 a.m.u, respectively. The dimension of the whole Fe-LBE system is $63.2\times63.2\times63.2$ Å^3. To calculate $D(T)_{0wt\%}$ we ran several simulations at elevated high temperatures: 750 °C, 775 °C, 800 °C, 825 °C, 850 °C, 875 °C, 900 °C, 925 °C, 950 °C, 975 °C and 1000 °C. The Moldy control parameters of simulation are: NPT ensemble, Anderson zero constant pressure, time step (dt) of 0.0001 ps and 100000 steps of MD simulation. After simulations, $D(T)_{0wt\%}$ was calculated using equations (6), (7) and (7). To validate the results we compared to available experimental data as reported by Zhang and Li [5]. The validated simulation model then will be used for next simulation.

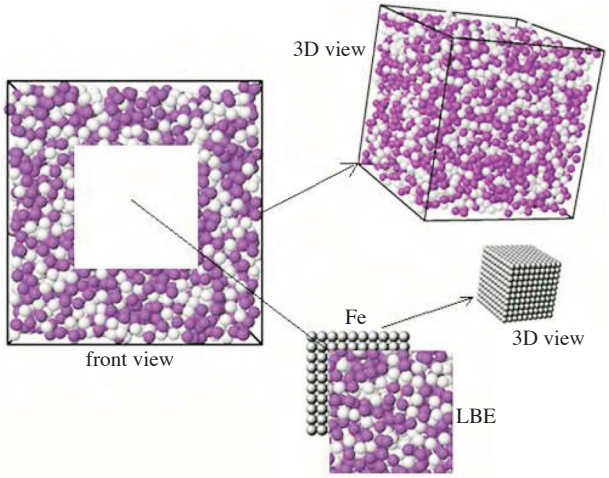

Figure 1. Model of corrosion simulations (Jmol visualization code, at http://www.jmol.org).

3.2. Determination of oxygen content

The second simulation injects the oxygen atoms into LBE coolant to reduce the corrosion. As reported by experiments [3–5], the oxygen content is very small compared with the coolant material. Then we need to make adjustment to our simulation model in order to close to experiment. We expand our size of simulation model in order to get better results. The FeO(LBE) system has dimension $123 \times 124 \times 125$ Å^3 where the iron bcc bulk is still placed in the center of the system and the oxygen atoms are inserted and distributed evenly in LBE with certain wt%. The number of iron atom is 10745 and the LBE coolant is composed from 20027 (44.3 wt%) lead atoms and 24979 (55.7 wt%) bismuth atoms. The simulation temperature is the same in each case, 750 °C, but with different oxygen content: 226 atoms (0.0386 wt%), 340 atoms (0.0581 wt%), 450 atoms (0.0768 wt%), 674 atoms (0.115 wt%), 906 atoms (0.155 wt%), 1132 atoms (0.193 wt%) and 1348 atoms (0.230 wt%). The atomic mass of oxygen is 15.998 a.m.u. The consideration of using a fixed single temperature 750 °C in the simulations is in order to be able to check with available experimental data that have been reported by Zhang and Li [5]. This is also to accommodate the abnormal condition of fast reactor accident where it can be about 750 °C as we state in introduction section [18]. The second simulation should be able to predict the proper oxygen content for significant and effective reduction of iron corrosion by evaluating the RDFs, MSD, D, and microstructure pictures (plot of coordinates) of iron. The Moldy control parameters are similar to section 3.1, but with 160000 MD step or 16 ps in time.

3.3. Iron diffusion calculation with oxygen content

The results obtained from second simulation bring leads to the prediction that a proper oxygen content leads to significant reduction of corrosion rate. The purpose of the third simulation is to calculate the iron diffusion $D(T)$ after oxygen injection. These simulations are similar to the FeLBE system as described in Section 3.1, however with the proper oxygen content injected. All simulations have same proper oxygen-content, based on conclusion of second simulation result, but with different temperatures.

4. Simulation results

4.1. First simulation

From the first simulation we calculate the diffusion coefficient of iron in LBE without oxygen injection using equations (6)–(8). In Figure 2, the $\log D(T)$ data were plotted against $1/T$. The plot of data shows a linear

graph with correlation coefficient R^2 of 0.984 and can be described by the relation

$$\log D\,(T) = -1020.699\frac{1}{T} - 7.277. \tag{9}$$

Using this equation the temperature dependence of diffusion coefficient of iron in LBE (without oxygen) can be expressed as

$$D\,(T)_{0\text{wt}\%} = 5.280 \times 10^{-8}\exp\left(2340.179/T\right) \quad [m^2 s^{-1}]. \tag{10}$$

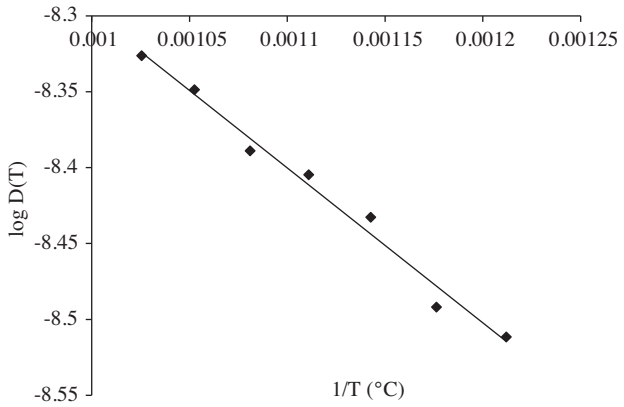

Figure 2. The plot of $\log D$ versus $1/T$ results from Fe in LBE simulation. The linear graph has correlation coefficient $R^2 = 0.984$.

4.2. Second simulation

The plots of MSD, RDF and diffusion coefficient of iron for different oxygen content are shown in Figures 3, 4 and 5, respectively. From Figure 3, showing the MSD curves, we see that a small oxygen injection can induce a reduction in corrosion rate. From Figure 4, showing the RDF curves, we know that the injection of oxygen maintained the stability of solid phase iron. A clear conclusion is derived from Figure 5, showing the diffusion coefficient. Here, there is a narrow range where the corrosion rate is very low and stable. This range is limited by two threshold numbers, the lower limit, 0.0768 wt%, and the upper limit, 0.155 wt%. Injecting oxygen more than 0.155 wt% can precisely stimulate the appearance of high corrosion again. Analysis of curves in Figures 3, 4 and 5 strongly suggests there is an optimal oxygen content which will significantly, stably and effectively slow the corrosion rate. The injection of oxygen content between of 0.0768 wt% and 0.155 wt% will be a good treatment to reduce high iron corrosion significantly and effectively.

4.3. Third simulation

In third simulation, 0.0768 wt% of oxygen is added to LBE coolant. Then we run simulations of the FeO(LBE) system for several elevated temperatures as discussed in Section 3.1. The plot of $\log\ D(T)$ versus $1/T$, obtained from the simulation, is shown in Figure 6.

5. Discussion

5.1. Simulation results

Some important results have been achieved in the present work. The diffusion coefficient of iron at 750 °C can be calculated using equation (10):

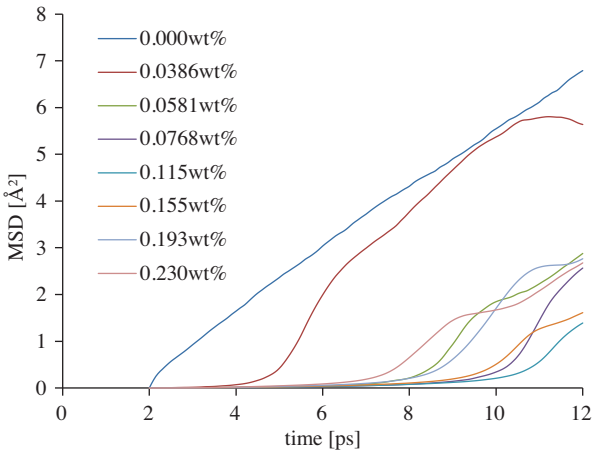

Figure 3. The MSD curves of iron for different oxygen contents. Note that oxygen content above 0.0581 wt% drastically reduces the iron diffusion.

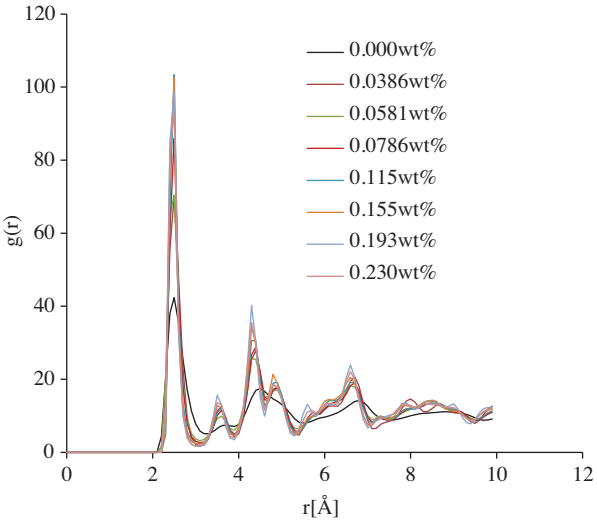

Figure 4. The RDF functions for iron in LBE. The lowest curve (black) is for the condition without oxygen injection and showing a liquid trend. With oxygen injection into LBE the RDFs show a solid trend.

$$D\left(T=750C\right)_{0\%wt.}=2.331\times10^{-9}\quad\left[m^2s^{-1}\right]. \tag{11}$$

Zhang and Li communicated that S. Banerjee, from his experimental work, reported that the diffusion coefficient of iron in LBE at temperature 750 °C is $2.27\pm0.11\times10^{-9}$ m^2s^{-1}, which means the diffusion coefficient is in the range of $(2.16–2.38)\times10^{-9}$ m^2s^{-1} [5]. Then our calculation, as shown in equation (11), lies perfectly within this range. Thus the simulation result is in a good agreement with the experimental result at temperature 750 °C. Then we consider that we can use our corrosion model in this work for further study of lead-bismuth eutectic corrosion.

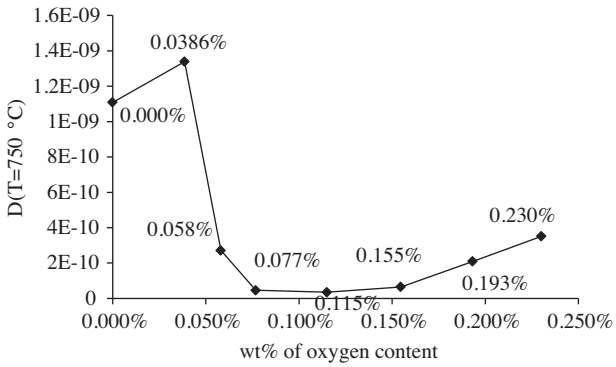

Figure 5. The iron diffusion coefficient in LBE for different oxygen content. By using equation (7) we develop a clearer conclusion that injecting of 0.0768 wt% oxygen has reduced the iron corrosion significantly and efficiently.

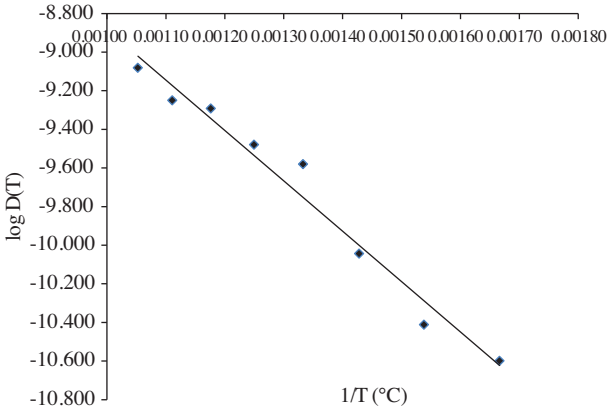

Figure 6. Plot of $\log D$ versus $1/T$ for iron diffusion by injection of 0.0768 wt% oxygen. The line is fit to the equation $\log D\left(T\right)=-\frac{2680.743}{T}-6.275$ and $R^2=0.972$.

In Figure 3, the lower MSD curves indicate low diffusion (or corrosion) rates. The RDF curves of Figure 4 can give a description of the material phase. Under conditions without oxygen injection the iron component has been brought to the non-solid phase condition as a result of interaction with LBE atoms. The iron component has been pushed to experience high corrosion. We can see from Figure 4, after injection of oxygen, the RDF curves show a characteristic indicating a trend toward solid phase condition. A very clear conclusion is from Figure 5. We can see the injection between 0.0768 wt% and 0.155 wt% will lower the corrosion to the lowest and most stable level.

The temperature-dependent diffusion coefficient of iron $D(T)$ at 0.0768wt% oxygen content was calculated in the third simulation. The result is shown in Figure 6, via plot of $\log D$ versus $1/T$. We can derive from this graph that the temperature-dependent diffusion coefficient of iron is

$$D\left(T\right)_{0.0768\%wt.} = 5.312 \times 10^{-7} \exp\left(5981.124/T\right) \quad \left[m^2 s^{-1}\right]. \tag{12}$$

Figure 7 shows a comparison between $D(T)_{0\ wt\%}$ and $D(T)_{0.0768\ wt\%}$. Figure 8 shows the microstructure of iron for different weight-fractions of oxygen. Figure 8a shows a microstructure of iron before simulation, that is the bcc crystal. The microstructure of iron after 160000 simulation steps without oxygen issue is shown in Figure 8b, describing the high corrosion condition of iron at 750 °C. A fascinating picture is shown in Figure 8c, for an injection of 0.0586 wt% oxygen. Note that the iron structure has started to stabilize from high corrosion. Figures 8d–8f show the performance of iron with 0.0786–0.155 wt% oxygen injection at 750 °C, that they exhibit very low corrosion. The structure of iron is relatively stable as a solid bcc crystal, primarily for Figure 8e. However, a slightly accelerated corrosion appears for injection of 0.193 wt% in Figure 8g. We can calculate the fractional reduction of diffusion (corrosion) via the following equation:

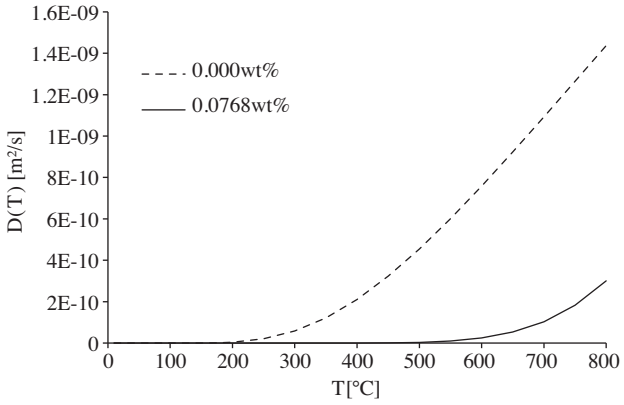

Figure 7. The comparison of $D_{0.076\ wt\%}$ and $\mathrm{D}_{0.00\ wt\%}$ of iron corrosion reduction. The corrosion rate has been reduced significantly by 0.0768 wt% of oxygen injection.

$$\%Reduction(T) = \frac{D_{0\ wt\%}(T) - D_{0.768\ wt\%}(T)}{D_{0\ wt\%}(T)}. \tag{13}$$

Figure 9 shows the plot of equation (13) for various simulation temperatures, using equations (10) and (12). We can see that the reduction at temperature 550 °C and 750 °C is 98.66% and 92.16%, respectively. So, for lower temperature then, the corrosion of iron tends to decrease as well.

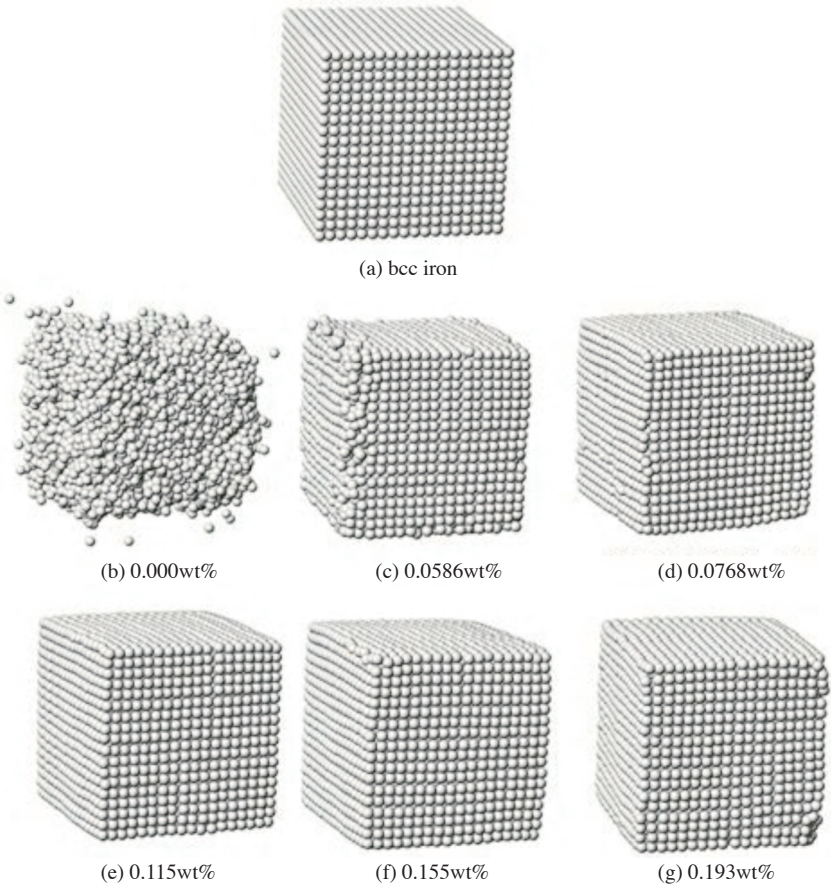

Figure 8. Microstructure of iron in LBE (a) before simulation; (b) after 160000 steps (or 16 ps) of MD integration without oxygen injection; (c–g) after 160000 steps (or 16 ps) of simulation with oxygen injection. Visualization with Jmol (http://www.jmol.org).

5.2. Review on the oxides formation

The LBE coolant is aggressive to the structural material due to the high solubility of elements of material (such as Fe, Ni and Cr) [7, 9, 18, 26, 29]. The injection of oxygen into LBE is believed to provide a partial barrier to metal dissolution by the formation of protective oxide scales/layers/films on the metal surfaces. The range of possible oxygen concentrations/contents is regulated by the necessity to establish a protective oxide scale and to avoid liquid metal oxides precipitation [29]. Figure 10 shows the division of corrosion area of iron in LBE, for temperature 750 °C.

From simulation results, a clear trend (see Figures 5 or 10) is observed in that the degradation of iron is decreased drastically and stable following an oxygen injection of 0.0768 wt% (lower limit), subsequently forming a stable protective oxide film in the solution. The stability of lowest corrosion can be maintained to the upper limit of fractional injection, 0.155 wt%. In this way, a useful range of oxygen content in a system containing LBE is advised; that is defining a lower limit (0.0768 wt%), where the development of magnetite is guaranteed and an upper limit (0.155 wt%) leads to the precipitation of lead oxide [29]. Within this range the protectiveness of the oxides can vary as a function of the structural material composition [29]. From a thermodynamics point of view, the injection of 0.0768 wt% oxygen provides a sufficient potential to develop a stable magnetite layer on

the material surface. In general, the lower limit for the oxygen content is defined by the stability of protective oxides, such as magnetite oxides (Fe_3O_4), while the higher limit (upper limit) is established by the precipitation of coolant oxide, for example PbO [29]. The precipitation of liquid metal oxides PbO is not desirable due to the risks of erosion and clogging. The range of oxygen content between lower limit and upper limit seems to be able to provide a longer protection to the alloy from corrosion. The upper limit of oxygen avoids the contamination by coolant oxides. The lower limit of oxygen enhances the corrosion protection by the self-healing oxide layer which depends on the structural material [27]. The main oxide formed in LBE coolant is lead monoxide (PbO) as it is the most stable oxide when compared to other lead oxides and bismuth oxides [27].

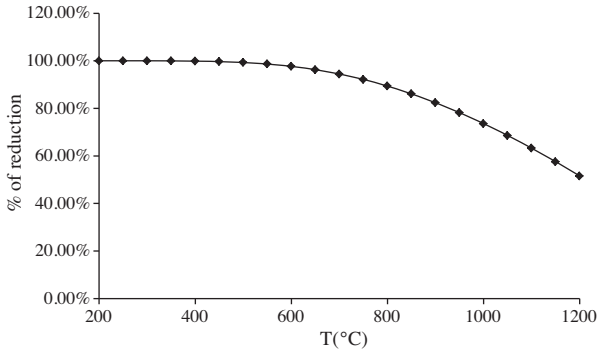

Figure 9. Plot showing reduction of diffusion rate after injection of 0.0768 wt% of oxygen. At 750 °C temperature the diffusion (corrosion) rate is reduced to about 92.16%.

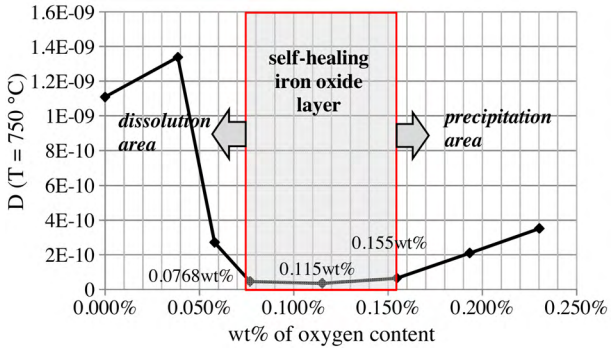

Figure 10. The three areas of corrosion for iron in LBE: dissolution area, self-healing iron oxide layer area and precipitation area.

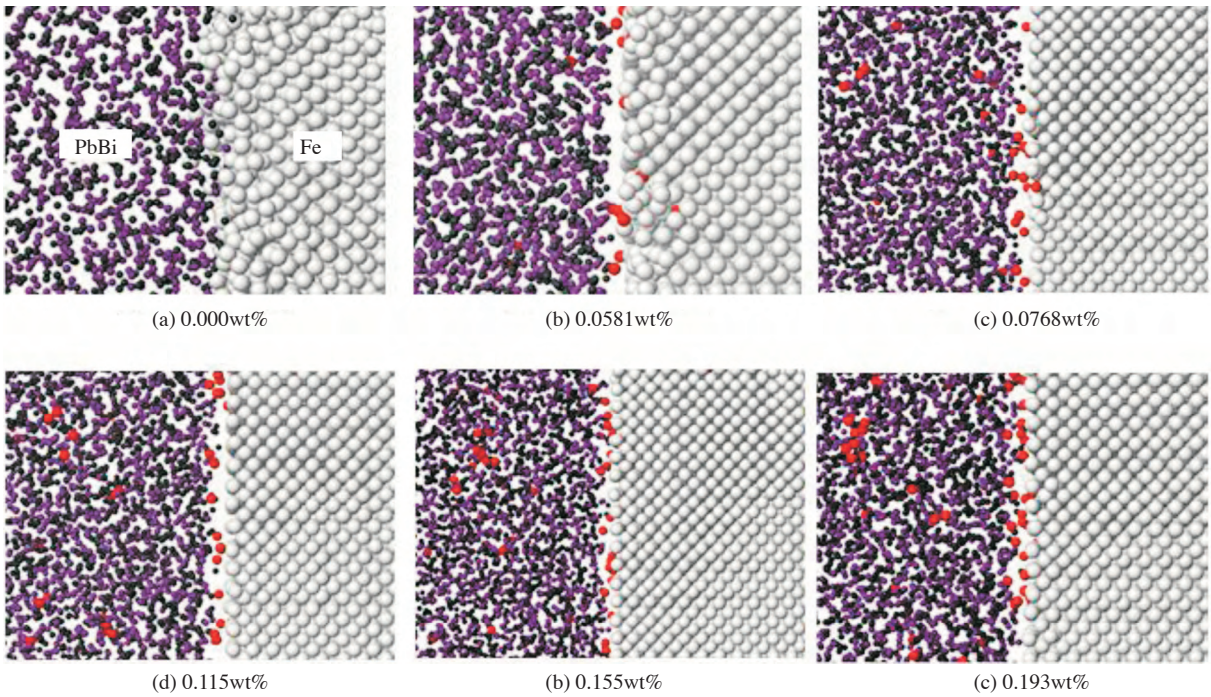

Figure 11. The microscopic views of Pb atoms, Fe atoms and oxygen atoms for various wt% of oxygen injection after MD simulation at 750 °C. Figure (a) is without oxygen injection. Visualization constructed with Jmol (http://www.jmol.org).

From theoretical point of view it is possible to promote protective oxide film by assuring that the oxygen potential in the liquid metal is above the potential for film formation on the structural material in the high temperature range ($> 450\ ^\circ$C) [27]. Our simulation (Figure 10) shows we have three different corrosion regimes as function of oxygen concentrations. When the oxygen content is too low (< 0.0768 wt%) the dissolution of iron nonetheless occurs. At higher oxygen contents (> 0.155 wt%) oxidation occurs, which results in the degradation of the structure and/or the formation of Pb oxides. Between these two extremes there exists a narrow transition region where the kinetics transition between dissolution and oxidation and the overall reaction rate is kept very small [27]. From the point of view of active oxygen control then the lower oxygen limit is firstly determined by the relative thermodynamic stability of the oxide when compared to the Pb oxide, the more stable the lower the oxygen potential, and the largest operational temperature range [27].

Iron is oxidized when it is immersed in molten LBE containing sufficient oxygen [7]. The amount of oxygen which is needed is determined by temperature and the corresponding free energy of formation of the oxide. The Ellingham diagram is a plot of the free energies of formation of various oxides, plotted against temperature and with the nomograph to calculate the corresponding partial pressure of oxygen for various points on the plot. On this plot, if the state of the LBE (corresponding to temperature and oxygen content) is above the line for a particular oxide, then that oxide is thermodynamically stable and can form, given the proper chemical kinetics [7]. On the contrary, if the state of the LBE is below the line, then that oxide cannot form (regardless of kinetics). According to this Ellingham diagram then the oxygen content of the LBE can be set, for a given temperature, to be below the PbO line such that neither the lead nor the bismuth in LBE can be oxidized; yet the LBE can still have enough dissolved oxygen to oxidize the iron, since the line for this element is below the lines for lead and bismuth oxides [7]. As this study is a preliminary study then we confine our work to analyze the lower and upper limit of oxygen content based on the simulation result. We do not explore the Gibbs free energy from simulation results, but do intend to examine it in subsequent work.

Now we discuss and see the microscopic view of the structure of materials, PbBi coolant, iron and oxygen. Figure 11 visualizes why the high corrosion of iron can be reduced by oxygen. Figure 11a shows that without oxygen injection, Pb and Bi atoms near enough to iron will interact strongly with Fe atoms at iron surfaces. Many Pb and Bi atoms can penetrate the surface of iron, causing high degradation or corrosion. However, injecting 0.0581 wt% of oxygen into LBE seems to start to create a very narrow barrier that separates the LBE atoms, Pb and Bi, and Fe atoms at their surfaces (Figure 11b). The iron oxide layer starts to develop to maintain the bcc structure of iron from LBE attack. However with this amount of oxygen injection the corrosion is still relatively high at the surface of iron (Figure 11b). The injection of oxygen in the range of 0.0768–0.155 wt% seems to be able to develop a stable iron oxide layer to protect the structure of bcc continuously (see Figures 11c–e). However, increasing the oxygen content of injection (to more than 0.155 wt%) seems to start the precipitation process that stimulates more corrosion. Figure 11f shows injection of 0.193 wt% oxygen that results in a precipitation. Many oxygen atoms assembled together with Pb atoms that may develop the PbO oxide. Figure 8e has also confirmed the degradation of iron for 0.193 wt% injection of oxygen. The iron oxide layer has been scrapped by LBE coolant. Soontrapa and Chen [16, 17] have also investigated the MD method about the formation of magnetite (Fe_3O_4). They used the advanced potential of EAM type to interact among the metal atoms. They can also show the formation of iron oxide layer nicely. However they did not study the effect of oxygen injection with various contents. In our simulation at least we can show that there are three areas of iron corrosion.

Now we discuss and compare to the experimental results. The paper by Kurata and Saito [30] shows that

there is a correlation between oxygen content and temperature for steel in LBE. To maintain the protective oxide layer, the oxygen content must be increased at LBE higher temperature. They have reported that the corrosion of 316SS steel was reduced using oxygen injections of 3.2×10^{-4} wt% at 450 °C, 6.3×10^{-4} wt% at 500 °C, 1.2×10^{-3} wt% at 550 °C, and 2.0×10^{-3} wt% at 600 °C. This result was also reported by Soler et al. [31], in which they experienced corrosion reduction of T91 martensitic steel in lead-bismuth eutectic by injecting 2.0×10^{-3} wt% at 600 °C. In the present work, protection was achieved with 7.68×10^{-2} wt% oxygen injection in LBE at 750 °C. Looking at those experimental results, we assume that our work and results are in agreement for temperature 750 °C. In addition, we investigated the iron material and not steel. There is also the experimental data of EP823 steel corrosion in liquid lead [32]. The corrosion reduction was studied by injecting oxygen at about 10^{-3} wt% at 700 °C. Zelenskii et al. [3] also studied the 15Kh12MS2AG steel in liquid lead at 750 °C, using an oxygen injection of 1.9×10^{-2} wt% to reduce the corrosion. Lead oxide PbO was introduced into the lead to ensure constant oxygen content in lead during the test at the level of 1.9×10^{-2} wt%. After testing, a barrier layer is oxide created that prevents high corrosion [3]. Steel was used, not iron, with a coolant using molten lead. The test of corrosion-resistant steel in LBE have also been reported by Rivai and Takahashi [13], using novel steel Al-SUS304-sputtering-coated HCM12A that introduced 2×10^{-5} wt% oxygen content at the high temperature 800 °C. So, the oxygen content seems also to be influenced by the quality of the steel as well as the temperature.

6. Conclusion and suggestion

The study of iron corrosion reduction in LBE coolant by molecular dynamic method has been successfully studied. We found that the diffusion coefficient of iron in molten LBE was $D\left(T\right)_{0\mathrm{wt\%}} = 5.280\times10^{-8}\exp\left(2340.179/T\right)$ $\mathrm{m^2\,s^{-1}}$ without oxygen content. Significant and effective reduction of iron corrosion can be achieved by injection of about 7.68×10^{-2} wt% of oxygen atoms into LBE coolant for starting the development of protective oxide. The oxygen injection of more than 1.55×10^{-1} wt% will induce high corrosion, on the contrary. From microstructure of the iron, we can see the injection of (7.68×10^{-2}–1.55×10^{-1} wt%) oxygen atoms seem to be able to stabilize the iron structure significantly. The temperature dependence of the diffusion coefficient of iron has been reduced to $D\left(T\right)_{0.0768\mathrm{wt\%}} = 5.312\times10^{-7}\exp\left(5981.124/T\right)$ $\mathrm{m^2\,s^{-1}}$ with oxygen content of 7.68×10^{-2} wt%. Taking the value of the iron diffusion coefficient at 750 °C, we see that there is a significant reduction of iron corrosion to about 92.16% with injection of 0.0768 wt% oxygen; and at temperature 550 °C we have reduction of about 98.66%. Comparison of experimental results with our work also show there are three regions of corrosion: a high corrosion region below the lower limit of oxygen content (7.68×10^{-2} wt%) for dissolution of iron; a high corrosion region above the upper limit of oxygen content (1.55×10^{-1} wt%) for precipitation of coolant oxides; and a very narrow corrosion region with self-healing stable protective oxide layers between lower limit and upper limit. For better results we suggest doing a larger scale simulation (on the order of millions of atoms) using MD parallel simulation, and also developing or using a better potential function of metal atomic interactions.

References

[1] B. B. Alchagirov, T. M. Shamparov, A. G. Mozgovoi, *High Temp.*, **41**, (2003), 210.

[2] A. M. Azad, *J. Nucl. Mater.,* **341**, (2005), 45.

[3] G. K. Zelenskii, A. G. Ioltukhovskii, M. V. L. Smirnova, I. A. Naumenko, S. A. Tolkachenko, *Metal Sci. Heat Treat.*, **49,** (2007), 11.

[4] D. Sapundjiev, S. Van Dyck, W. Bogaerts, *Corrosion Sci.,* **48,** (2006), 577.

[5] J. Zhang, N. Li, *J. Nucl. Mater.,* **373,** (2008), 351.

[6] A. Z. Kashezhev, M. Kh. Ponegev, V. A. Sozaev, A. I. Khasanov, A. G. Mozgovo, *High Temp.*, **8,** (2010), 756.

[7] A. M. Bolind, PhD Thesis, Nuclear Engineering, University of Illinois at Urbana-Champaign, Urbana, Illinois, 2009.

[8] A. K. Rivai, M. Takahashi, *J. Nucl. Mater.*, **398,** (2010), 139.

[9] J. Konys, H. Muscher, Z. Voß, O. Wedemeyer, *J. Nucl. Mater.*, **296,** (2001), 289.

[10] B. F. Gromov, Yu. S. Belomitcev, E. I. Yefimov, M. P. Leonchuk, P. N. Martinov, Yu. I. Orlov, D. V. Pankratov, Yu. G. Pashkin, G. I. Toshinsky, V. V. Chekunov, B. A. Shmatko, V. S. Stepanov, *Nucl. Eng. Design,* **173,** (1997), 207.

[11] A. K. Rivai, T. Kumagai, M. Takahashi, *Prog. Nucl., Energy*, **50,** (2008), 575.

[12] Y. Kurata, M. Futukawa, S. Saitu, *J. Nuc. Mater.,* **373,** (2008), 164.

[13] Y. N. Wu, L. P. Wang, Y. S. Huang**,** D. M. Wang, *Chem. Phys. Lett.,* **515**, (2011), 217.

[14] A. Arkundato, Z. Suud, M. Abdullah, *AIP Conf. Proc.,* **1244,** (2010), 136.

[15] A. Maulana, S. Zaki, K. D. Hermawan, Khairurrijal, *Progress in Nuclear Energy*, **50** (2008), 616.

[16] C. Soontrapa, Y. Chen, *Comput. Mater. Sci.*, **46**, (2009), 887.

[17] C. Soontrapa, Y. Chen, *Comput. Mater. Sci.*, **50**, (2011), 3271.

[18] A. K. Rivai, M. Takahashi, *J. Nucl. Mater.*, **398**, (2010), 139.

[19] A. K. Rivai, M. Takahashi, *Prog. Nucl. Energy*, **50**, (2008), 560.

[20] S. Zhen, G. J. Davies, *Phys. Status Solidi A*, **78,** (1983), 595.

[21] E. W. Lemmon, R. T. Jacobsen, *Int. J. Thermophysics*, **25**, (2004), 21.

[22] D. K. Belashchenko, O. I. Ostrovskii, *Russ. J. Phys. Chem.*, **80,** (2006), 509.

[23] K. Refson, *Comput. Phys. Commun.*, **126,** (2000), 309.

[24] G. J. Ackland, K. D'Mellow, S. L. Daraszewicz, D. J. Hepburn, M. Uhrin, K. Stratford, *Comput. Phys. Commun.*, **182,** (2011), 2587.

[25] W. D. Manly, *Corrosion*, **12,** (1956).

[26] T. Furukawa, G. Muller, G. Schumarcher, A. Weisenburger, A. Heinzel, F. Zimmermann, K. Aoto, *J. Nucl. Sci. Tech.*, **41(3)**, (2004), 265.

[27] OECD/NEA, Handbook on lead-bismuth eutectic alloy and lead properties, materials compatibility, thermal hydraulics and technologies, Edition 2007, (Nuclear Energy Agency, 2007), p.129. www.oecd-nea.org/science/reports/2007/pdf/chapter4.pdf accessed on march 21, 2012.

[28] A. Y. Kurpyazhkin, A. N. Zhiganov, D. V. Risovany, K. A. Nekrassov, V. D. Risovany, V. N. Golovanov, *J. Nucl. Mater.*, **372**, (2008), 233.

[29] A. Doubkova, D. Karnik, F. Di Gabriele, The influence of the oxygen content on the metal loss of the austenitic steel 17246 (AISI 321) in flowing liquid lead-bismuth eutectic. Accesse on June 01, 2012 from http://nuklear-server.ka.fzk.de/OFMS/
Web%2fMain%2fPublications%2f2006%2fDEMETRA%2fP_A.Doubkova_JournNuclMat_2006.pdf.

[30] Y. Kurata, S. Saito, *Mater. Transactions*, **50**, (2009), 2410.

[31] L. Soler, F. J. Martín, F. Hernández, D. Gómez-Briceño, *J. Nucl. Mater.,* **335**, (2004), 174.

[32] G. K. Zelenskii, Yu. A. Ivanov, A. G. Ioltukhovskii, I. A. Naumenko, I. A. Shkabura, *Metal Sci. Heat Treat.*, **48,** (2006), 412.